Ring-shaped Calorimetry Information for a Neural Egamma Identification with ATLAS Detector

João Victor da Fonseca Pinto[1], on behalf of ATLAS Collaboration
Federal University of Rio de Janeiro, Rio de Janeiro, Brazil
E-mail: joao.victor.da.fonseca.pinto@cern.ch

Abstract. This article presents the identification process of electrons based only on calorimeter information. It is based on the usage of ring-shaped description for a region of interest of the calorimeter which explores the shower shape propagation throughout the ATLAS calorimeters. This information is fed into a multivariate discriminator, currently an artificial neural network, responsible for hypothesis testing. The concept is evaluated for online selection (trigger), used for reducing storage rate into viable levels while preserving collision events containing desired signals. Preliminary results from Monte Carlo simulation data indicate that the background rejection can be reduced by as much as 50 % over the current method used in the High-Level Trigger, allowing for high-latency reconstruction algorithms such as tracking to run at a later stage of the trigger.

ATL-DAQ-PROC-2016-007
31/03/2016

1. Introduction

Succeeding the discovery of the Higgs boson in 2012 during Run 1, the LHC has started a new data-taking period (Run 2). During the run start-up in 2015, it successfully increased the energy in the center-of-mass of proton-proton collision physics to 13 TeV and shrank bunch spacing to 25 ns. Also, an increase of the luminosity is foreseen, targeting $1.6 \times 10^{34} cm^{-2} s^{-1}$, which will result in pile-up conditions of 44 mean inelastic interactions per bunch crossing. These changes in experimental conditions bring a proper environment for possible new physics discoveries and measurements.

ATLAS [1] is the largest LHC detector and was designed for a large spectrum of physics studies. Many physics channels have electrons in their final states. For electron identification, the calorimeter system plays a major role. In ATLAS, the calorimeter system comprises both electromagnetic (EMCal) and hadronic (HCal) sections, where the latter envelopes the electromagnetic counter-part. In the central region, the EMCal Barrel and both EMCal and HCal End-Cap employ a Liquid Argon and absorber technology. The central HCal is based on steel absorber with plastic scintillators.

These calorimeters consists of, for most of the η[2] acceptance, three samplings along longitudinal (depth) segmentation. Additionally, each sampling layer has its own lateral ($\eta \times \phi$)

[1] Speaker.

[2] ATLAS uses a right-handed coordinate system with its origin at the nominal interaction point (IP) in the centre of the detector and the z-axis along the beam pipe. The x-axis points from the IP to the centre of the LHC ring, and the y-axis points upward. Cylindrical coordinates (r, ϕ) are used in the transverse plane, ϕ being the azimuthal angle around the z-axis. The pseudorapidity is defined in terms of the polar angle θ as $\eta = -\ln \tan(\theta/2)$.

granularity, which may vary with η. The EMCal is complemented by a presampler (PS) within $|\eta| < 1.8$.

The ATLAS trigger system [2] aims at providing online selection of promising bunch crossing events into a viable output rate for recording and further offline processing. A set of improvements and upgrades have been made to address the new circumstances in the Run 2 (cf. Ref. [3] for trigger related upgrades).

The trigger operates applying selection chains (referred to as chains for simplicity), in which each selection level increases in latency and physics reconstruction depth. The first level (L1) is the start of the selection chain and it is hardware-based in order to achieve a latency of less than 2.5 μs meanwhile scaling down the readout rate to, at most, 100 kHz. Thereafter operates the High-Level Trigger (HLT), a software-based selection with average target latency of 550 ms and average output rate of 1 kHz. The physics selection menu consists of about $\sim$1000 chains out of which about $\sim$100 aims at selecting electron and photons signatures (referred to as EM particles).

2. Baseline Algorithm

The Egamma chain (Figure 1) is based on the Region-of-Interest (RoI) concept. The following short description emphasizes the particle identification (ID) task, which consists of disentangling the EM particles (signal) from collimated hadronic jets (background).

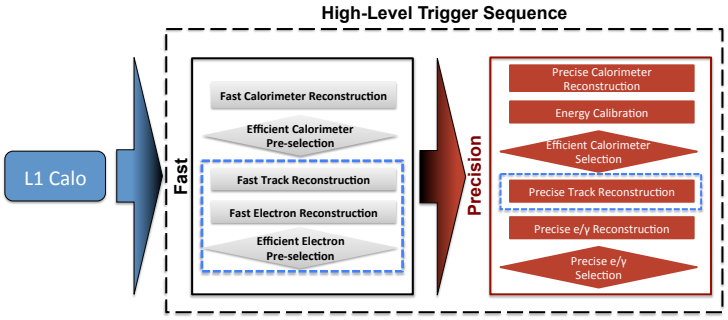

Figure 1: Flow diagram for the algorithm sequence of the Egamma chain. Steps surrounded by blue dashed lines only apply to electron chains.

A sliding window algorithm is used to build the L1 RoI, which is used to select EM objects by applying η-dependent E_{T} threshold and hadronic isolation requirements.

In the sequence, already in the HLT, fast reconstruction is applied to provide early rate reduction. Particularly for electron chains, the fast calorimeter and fast track reconstructions are combined to provide an efficient electron pre-selection. Calorimeter driven pre-selection is less resource intensive and, therefore, provides latency reduction. This reasoning is duplicated to the precision step where offline-like algorithms are applied.

The current algorithm used by Egamma ID makes extensive use of calorimeter shower shapes and widths, energy ratios, tracking quantities and track-cluster matching [4]. Offline reconstructed distributions of these discriminating quantities over Run 2 data can be found in Ref. [5].

Two standard selection variants are available. In cut-based ID, these quantities are individually compared to the respective optimized threshold. The likelihood (LH) ID variant, by contrast, uses a multivariate analysis technique, where a Naïve Bayes-like approach is applied over the very quantities (cf. Ref. [4] for more details on these variations). The LH ID variant is now the baseline method used on the precise calorimeter pre-selection and final selection for electrons as part of the Run 2 updates. Nevertheless, the fast stage still uses selection-based ID in which three, most discriminating, quantities are used by the calorimeter pre-selection.

3. Proposed Algorithm

The proposed algorithm (cf. Figure 2) aims at exploring the conic geometry of the shower shapes by using the cells of the calorimeter to build energy quantities describing the amount of energy available in each concentric ring around the cell of maximum energy deposition. This process preserves the lateral and longitudinal information of the shower shape and, thus, the physics interpretation, while reducing the amount of information with respect to using all cells.

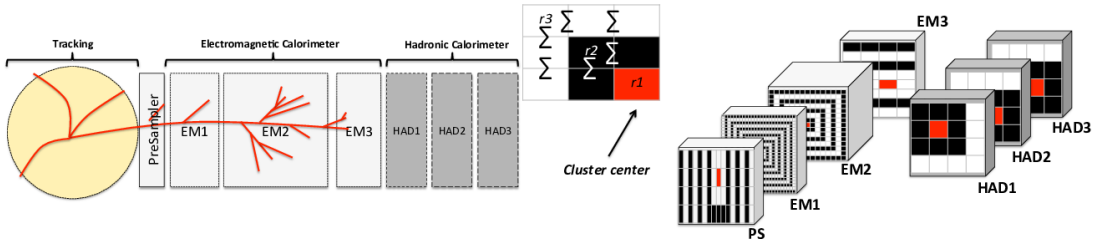

Figure 2: Sketches to illustrate the Ringer algorithm. Left: An EM shower propagation throughout the sampling layers of the calorimeters. Right: The calorimeter cells used to build the rings description over the calorimeters layers. The cell of first (central) ring is displayed in red, whereas the cells of the consecutive rings are alternated in black and white.

For the fast calorimeter pre-selection step, the Ringer RoI covers a region of the calorimeter, centered in the L1 provided RoI, of 0.4×0.4 in the $\eta \times \phi$ plane. The algorithm then starts on the second EM sampling layer (EM2)[3], where position (given in $\eta \times \phi$ plane) of the cell with highest E_{T} on the Ringer RoI is taken as the center of the cascade interaction with the calorimeter. The seed cell position is propagated to other calorimeter layers in order to define the axis of the rings in that layer ($c_{a,l}$). A ring $R_{n,l}$ contains all cells in a calorimeter layer l which are n cells from the axis. Formally,

$$R_{n,l} = \left\{ c_{n,l} \mid n = \left\lfloor \max\left(\frac{|\eta_{i,l} - \eta_{a,l}|}{h_{\eta,l}}, \frac{|\phi_{i,l} - \phi_{a,l}|}{h_{\phi,l}} \right) \right\rfloor, \forall c_{i,l} \in \Theta_{RoI,l} \right\}, \tag{1}$$

where (analogous to ϕ when suitable): $\eta_{i,l}$ and $\eta_{a,l}$ are respectively the $c_{i,l}$ and $c_{a,l}$ cells position in η; $h_{\eta,l}$ is the l^{th} layer granularity in η; $\Theta_{RoI,l}$ is the set of cells in the l^{th} layer which are within the Ringer RoI; $l \in \{\mathrm{PS}, \mathrm{EM1}, \mathrm{EM2}, \mathrm{EM3}, \mathrm{HAD1}, \mathrm{HAD2}, \mathrm{HAD3}\}$; and $n \in \{0, \ldots, N_l \mid N_{PS} = 7; N_{EM1} = 63; N_{EM2} = 7; N_{EM3} = 7; N_{HAD1} = 3; N_{HAD2} = 3; N_{HAD3} = 3\}$. If no cell is available for a given ring, the correspondent ring quantity is set to 0.

Sum of energies of cells in the ring over the sum of the cells energies in all rings form a vector of discriminating quantities. They are ordered outwards and from the innermost layer of the calorimeter and provided to a multivariate technique.

These discriminating quantities are fed into neural network (NN) [6] which performs the selection task. The architecture employed is a single hidden layer fully connected feedforward network (MLP — Multilayer Perceptron). The hidden and output layer activation function is set to $\tanh(\cdot)$. The data is divided into two datasets: the training set (contains 60% of available data), in which the NN weights are adjusted; and the test set (remaining 40%), used to verify that NN specialization does not occur and to evaluate performance. The NN weights are initialized by the Nguyen-Widrow [7] algorithm and optimized by applying the resilient back-propagation algorithm [8]. In order to avoid convergence to local optima, a total of 100 initializations was employed. The figure of merit used to evaluate performance was the threshold applied to the NN output which maximizes the SP-index,

[3] This convention is used for all sampling layers, thus HAD1 stands for the first hadronic layer, HAD2 the second hadronic layer etc.

$$SP(\%) = \sqrt{\sqrt{P_D \cdot (1 - FR)} \cdot \left(\frac{P_D + (1 - FR)}{2} \right)} \times 100\%, \quad (2)$$

where: P_D is probability of detection; and FR is the background rejection or fake rate.

The thresholds were adjusted using the signal efficiency of the benchmark for regions of η and E_{T}. Statistical fluctuations from the dataset are estimated by employing the cross-validation technique [6] with 50 sorts over 10 uniformly spread subsets of both signal and background datasets. The number of neurons in the hidden layer is chosen by the application of both cross-validation performance and generalization capability as criteria.

The operation points and fluctuations, respectively in terms of P_D and F_R, of the Ringer algorithm for each η region, when $E_{\mathrm{T}} < 30$ GeV, are of: 96.9 ± 0.1 and 4.6 ± 0.2 ($0 \leq |\eta| < 0.8$); 96.9 ± 0.1 and 4.6 ± 0.2 ($0.8 \leq |\eta| < 1.37$); 90.7 ± 0.1 and 6.2 ± 1.2 ($1.37 \leq |\eta| < 1.54$); 95.1 ± 0.1 and 10.9 ± 1.2 ($1.54 \leq |\eta| < 2.5$). The region $1.37 \leq |\eta| < 1.54$ is the transition between the barrel and end-cap calorimeters, where deterioration of the response of the detector occurs.

When $30 \leq E_{\mathrm{T}} < 50$, these values are the following: 99.0 ± 0.1 and 5.5 ± 0.7 ($0 \leq |\eta| < 0.8$); 99.1 ± 0.1 and 6.3 ± 0.9 ($0.8 \leq |\eta| < 1.37$); 95.9 ± 0.1 and 9.5 ± 2.1 ($1.37 \leq |\eta| < 1.54$); 97.5 ± 0.1 and 11.2 ± 0.9 ($1.54 \leq |\eta| < 2.5$).

Finally, for higher energies ($E_{\mathrm{T}} \geq 50$ GeV): 99.4 ± 0.1 and 2.0 ± 0.4 ($0 \leq |\eta| < 0.8$); 99.7 ± 0.1 and 5.2 ± 1.0 ($0.8 \leq |\eta| < 1.37$); 96.7 ± 0.1 and 2.7 ± 1.9 ($1.37 \leq |\eta| < 1.54$); 98.4 ± 0.1 and 4.7 ± 0.9 ($1.54 \leq |\eta| < 2.5$).

4. Results

The proposed algorithm, based upon ring-shaped calorimetry description, was compared to the baseline algorithm executed in the fast calorimeter pre-selection step. The selection chain of the trigger aims to pick events containing at least one electron with $E_{\mathrm{T}} > 24$ GeV. Prompt electrons from $Z \rightarrow ee$ decays simulated using Monte Carlo were used as signal input and, for the background, a dataset contained simulated hadronic jets with $E_{\mathrm{T}} > 17$ GeV. Both datasets have pile-up emulation of 20 mean inelastic interactions per bunch crossing.

Only electrons reconstructed in the full offline processing were considered in the efficiency computation. Analysis is done only for the fast calorimeter pre-selection decision. Thus, if a candidate is discarded in advance by the L1 algorithm, it is simply not taken into consideration and does not count for efficiency measurement. Likewise, the behavior of the remaining selection of the electron chain was not evaluated.

Apart from meeting above conditions, the training data were selected as follow: signal data are particles from $Z \rightarrow ee$ dataset considered as electrons by the most exigent criteria of the offline LH ID; and background data are particles from hadronic jets dataset, where the residual contamination of prompt electrons is removed by using simulation predictions.

The preliminary results in Figure 3 show that the proposed algorithm can operate with similar performance over both the full η acceptance and over the range of the pile-up conditions. Efficiency measurements use tag-and-probe[4] (T&P) technique to allow comparison with other studies which also consider collision data efficiencies. Notwithstanding, the efficiency measurements demonstrate the capacity of a factor of 2 reduction in the background efficiency: the signal efficiency of the ringer approach remains almost unchanged ($97.6\% \rightarrow 97.7\%$) while the fraction of background surviving selection changes from $12.7\% \rightarrow 5.3\%$. Therefore, these results provide indication that the proposed algorithm is able to further improve Egamma HLT chain by upgrading the fast calorimeter pre-selection step.

[4] The tag-and-probe is a method to measure signal efficiency. $Z \rightarrow ee$ events with one electron passing default trigger and second (probe) reconstructed electron by offline are selected and used to check if probe electron has also passed trigger.

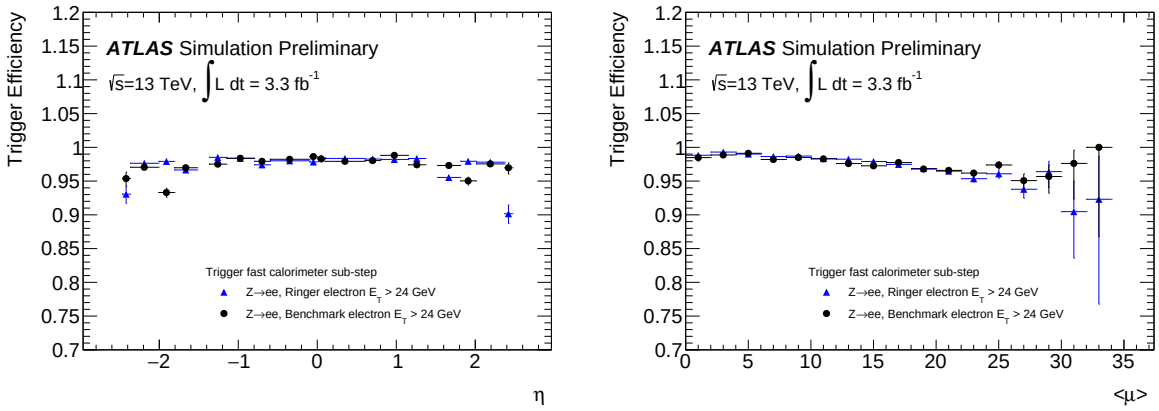

Figure 3: Electron T&P efficiency over $Z \rightarrow ee$ simulation data for the trigger fast calorimeter pre-selection. Left: as a function of the offline reconstructed electron candidates pseudorapidity (η). Right: as a function of the number of pile-up events (μ). Taken from Ref. [9].

5. Conclusions

A selection method for electrons using ring-shaped calorimetry information was described. It is an alternative for the fast calorimeter pre-selection stage of HLT trigger. Preliminary results from simulation data demonstrate that the algorithm is able to provide similar signal efficiency while improving background rejection by a factor of 2. Likewise, this gain also means a latency reduction due to background removal in early stages of the trigger chain. Also, the execution time of the proposed algorithm is equivalent to the baseline one. Hence, it may contribute to further improve the Egamma High-Level Trigger for ATLAS experiment. Finally, a version of the algorithm is being analysed on the offline reconstruction and it may also be applied to photon identification which relies on calorimeter information only.

6. Acknowledgements

We would like to thank CNPQ, CAPES, RENAFAE, FAPERJ (Brazil) and EU through the E-Planet project.

References

[1] ATLAS Collaboration 2008 *JINST* **3** S08003
[2] ATLAS Collaboration 2012 *Eur. Phys. J. C* **72** 1849 (*Preprint* `1110.1530`)
[3] ATLAS Collaboration 2013 Technical Design Report for the Phase-I Upgrade of the ATLAS TDAQ System Tech. Rep. CERN-LHCC-2013-018. ATLAS-TDR-023 CERN Geneva URL `https://cds.cern.ch/record/1602235`
[4] ATLAS Collaboration 2014 Electron efficiency measurements with the ATLAS detector using the 2012 LHC proton–proton collision data ATLAS-CONF-2014-032 URL `http://cdsweb.cern.ch/record/1706245`
[5] ATLAS Collaboration Electron shower shapes, tracking, isolation and invariant mass distributions from $Z \rightarrow ee$ and $J/\Psi \rightarrow ee$ events URL `https://atlas.web.cern.ch/Atlas/GROUPS/PHYSICS/PLOTS/EGAM-2015-003`
[6] Haykin S 1999 *Neural Networks: A Comprehensive Foundation* (Prentice Hall) ISBN 9780780334946
[7] Nguyen D and Widrow B 1990 *Proceeding of the International Joint Conference on Neural Networks* vol 3 (San Diego, USA) pp 21–26
[8] Riedmiller M and Braun H 1993 *Proceedings of the IEEE International Conference on Neural Networks* (San Francisco, USA) pp 586–591
[9] ATLAS Collaboration Expected performance of the ringer algorithm URL `https://twiki.cern.ch/twiki/bin/view/AtlasPublic/EgammaTriggerPublicResults`